crystals

MDPI

Article

The Role of Weak C–H···X (X = O, π) Interactions in Three 1-Hydroxy-2-naphthoic Acid Cocrystals with N-Containing Heteroaromatics: Structural Characterization and Synthon Cooperation

Huiqi Qu [1], Ruixin Chen [2,*], Yiru Ma [3], Na Li [3], Mingjuan Zhang [3], Yueqin Yu [3], Zhiguo Lv [1] and Kang Liu [3,4,*]

[1] College of Chemical Engineering, Qingdao University of Science and Technology, Qingdao 266042, China
[2] Department of Mathematics, College of Mathematics and Physics, Qingdao University of Science and Technology, Qingdao 266061, China
[3] Key Laboratory of Eco-Chemical Engineering, International Science and Technology Cooperation Base of Eco-Chemical Engineering and Green Manufacturing, College of Chemistry and Molecular Engineering, Qingdao University of Science and Technology, Qingdao 266042, China
[4] Chaofeng Steel Structure Group Co., Ltd., Hangzhou 311215, China
* Correspondence: mathcrx@163.com (R.C.); liukang82@126.com (K.L.)

Abstract: Herein, three novel cocrystals of 1-hydroxy-2-naphthoic acid: tetramethylpyrazine, 1-hydroxy-2-naphthoic acid:1,10-phenanthroline, and 1-hydroxy-2-naphthoic acid:1,4-bis(imidazol-1-ylmethyl)benzene (L2) were obtained by crystallization in methanol–water mixed solvent via a slow evaporation method. The cocrystalline products **1**−**3** were carried out by a range of techniques, including single-crystal X-ray diffraction, Fourier transform–infrared spectroscopy, elemental analysis, and thermogravimetric testing. We analyzed the crystal structures of the cocrystals **1**−**3** and found that weak interactions C–H···X (X = O or π) were of great importance in the process of self-assembly as well as strong and conventional hydrogen bonds (N–H···O, O–H···N, O–H···O), leading to a stable and diverse multidimensional supramolecular architecture. It is worth noting that a series of ring motifs with different sizes were explored in the crystal structures of the above complexes, such as $R^2_2(5)$, $R^2_2(7)$, $R^2_2(8)$, $R^2_3(13)$, $R^2_4(16)$, $R^4_4(16)$, $R^4_4(22)$, and so on. The classical and robust supramolecular synthon intermolecular bond between acid and pyridine (acid···pyridine) heterosynthon $R^2_2(7)$, commonly found in organic solids containing carboxylic acids with other N-containing heteroaromatics, was further demonstrated to be involved in the construction of the hydrogen-bond networks of cocrystal 1. The thermogravimetric technique used in this study proved that the mass losses of these three cocrystals were closely related to the strength of the hydrogen bonds in the package fraction.

Keywords: cocrystals; supramolecule; self-assembly; 1-hydroxy-2-naphthoic acid; synthon

check for updates

Citation: Qu, H.; Chen, R.; Ma, Y.; Li, N.; Zhang, M.; Yu, Y.; Lv, Z.; Liu, K. The Role of Weak C–H···X (X = O, π) Interactions in Three 1-Hydroxy-2-naphthoic Acid Cocrystals with N-Containing Heteroaromatics: Structural Characterization and Synthon Cooperation. *Crystals* **2023**, *13*, 402. https://doi.org/10.3390/cryst13030402

Academic Editor: Ana M. Garcia-Deibe

Received: 28 January 2023
Revised: 15 February 2023
Accepted: 22 February 2023
Published: 26 February 2023

Copyright: © 2023 by the authors. Licensee MDPI, Basel, Switzerland. This article is an open access article distributed under the terms and conditions of the Creative Commons Attribution (CC BY) license (https://creativecommons.org/licenses/by/4.0/).

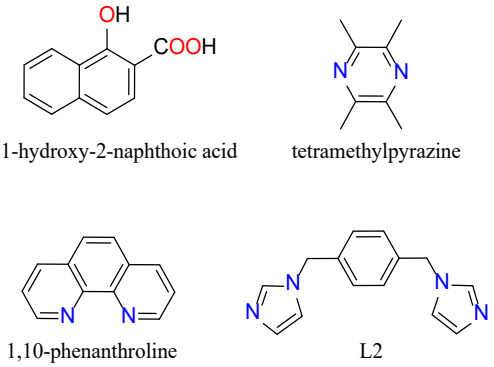
1. Introduction

In the past few decades, the synthesis of cocrystals have attracted much attention in the medical field and possess very bright development prospects in the field of future pharmaceutical research due to their potential application value. [1–6]. In the Indo–U.S. Bilateral Meeting, cocrystals, which represent a significant class of complexes, were redefined by Zaworotko et al. [7]. Typically, they are neither a solvent nor a simple salt, but a solid, usually composed of two or more distinct molecular or ionic compounds in a single crystalline phase with stoichiometric ratios. A detailed understanding of the role of various non-covalent intermolecular interactions is very important for the rational designing of cocrystals with ideal structural characteristics [8–13]. As one of the intermolecular interactions found in cocrystals, hydrogen bonding (HB) is the primary method for determining how molecules aggregate together to generate an organic solid. In addition, hydrogen

bonding plays a critical role in the ordering of molecules within organic solids, which may directly influence the physical and chemical properties of organic solids [14–21]. On the other hand, aromatic ring units also play an essential role in the process of self-assembly through aromatic stacking interactions, including π–π and C–H···π packing interactions, leading to abundant varieties of multidimensional supramolecular architectures [22–29]. Recently, some examples have been reported where interactions between aromatic stackings are significant in constructing crystalline materials. Sun et al. successfully designed and synthesized a new class of aromatic materials that tend to form layered π–π stacked crystalline materials. Their π–π interplane distance is 3.247 Å, which is 0.1 Å smaller than that of high-orientation pyrolytic graphite (HOPG). [30]. Nishio et al. presented evidence by systematically exploring the Cambridge Structural Database (CSD) for the idea that C–H···π interactions generally directly affect crystal packing and determine the structure of clathrates to a large extent. [31].

For the purpose of understanding and studying the noncovalent interfaces in organic crystals to a greater depth, the concept of supramolecular synthons was conceived, which was first suggested by Desiraju in 1995 [32]. The concept bears both chemical and geometrical information. Supramolecular synthons based on non-covalent interactions can be classified into two kinds, namely "heterosynthons" originating from the mutual recognition of two or more different but complementary functional groups. Some synthons are robust yet versatile, and they are repeated in different structures over a variety of complexes. Heterosynthons, which are key to the design of cocrystals, have been found to be more prevalent in cocrystals than homosynthons [33–37]. In past reports, the acid···pyridine bimolecular cyclic hydrogen-bonded heterosynthon $R^2_2(7)$ has been identified as a classical and robust supramolecular synthon, which is frequently formed between a carboxylic acid group and a pyridine group. Nangia and coworkers researched CSD and found that the occurrence probability of this motif is over 90% when the two competing functional groups are both absent, owing to its relatively low energies [38–44]. Except for the acid···pyridine synthon $R^2_2(7)$, common heterosynthons in the literature also include acid···amide, alcohol···pyridine, etc.

In a continuation of our studies to synthesize polycomponent organic solids of hydroxyl naphthoic acid with N-doped heteroaromatics, in this manuscript we describe three high-yielding novel cocrystals of 1-hydroxy-2-naphthoic acid with tetramethylpyrazine, 1,10-phenanthroline, and 1,4-bis(imidazol-1-ylmethyl)benzene (L2) (compound formulas exhibited in Scheme 1), which display diverse 3D-network supramolecular architectures. These cocrystals (**1**–**3**) were obtained through single-crystal X-ray diffraction, Fourier transform–infrared spectroscopy, elemental analysis, and thermogravimetric testing. In terms of their crystal structures, we discussed the role of the weak interactions C–H···X (X = O or π) and π−π aromatic stacking interactions in crystal engineering. In addition, we analyzed the supramolecular synthons found in the studied structures, which contained the classical and well-known synthons $R^2_2(7)$ and $R^2_2(8)$.



1-hydroxy-2-naphthoic acid tetramethylpyrazine

1,10-phenanthroline L2

Scheme 1. Chemical structure of co-formers discussed in this work.

2. Materials and Methods

2.1. General Materials and Physical Characterization

All the crystal formers (co-formers) (Scheme 1) and solvents used in this manuscript were purchased commercially and used directly without purification. L2 [1,4-bis(imidazol) dimethylbenzene] was obtained by referring to a previously reported procedure [45]. A Perkin-Elmer 2400 elemental analyzer was used for the trace analysis of carbon, hydrogen, and nitrogen elements. Fourier transform–infrared spectroscopy (FT–IR) measurements of complexes **1–3** was conducted on a Nicolet Impact 410 spectrometer. In addition, the complexes were prepared as KBr pellets within the scope of 4000–400 cm^{-1}. Absorptive intensities were expressed as follows: strong (s), medium (m), and weak (w), respectively, as discussed in the synthesis section. Thermogravimetric analysis (TGA) was conducted on a Perkin-Elmer TGA 7 analyzer to explore the thermal stability of all the cocrystals. All the cocrystals could be stable in air for a long time, and a TGA test was employed by using a purging nitrogen flow from room temperature to 900 °C with a heating rate of 10 °C/min. Thermal analysis of the samples was performed on a Thermal Advantage DSC Q200 device (TA Instruments, USA), which was calibrated for temperature and cell constants using high-purity indium (Aldrich Chemical Co. Inc.). Samples (3–10 mg) were crimped in non-hermetic aluminum pans, and an empty pan was used as a reference. The samples were heated from 0 to 300 °C at a heating rate of 10 °C/min and purged with dry nitrogen at 50 mL/min. All the measurements were performed in triplicate, and the heating curves were evaluated using the TA Instruments Universal Analysis 2000 Advantage software V5.5.3. Cocrystals **1–3** were grown from a 1:1 methanol–distilled-water mixture via slow evaporation under ambient conditions. The molar ratio of 1-hydroxy-2-naphthoic acid to each co-former was 1:2, 1:1, and 2:1, respectively. The detailed crystal preparation steps were as follows.

2.2. Syntheses of the Complexes **1–3**

1-hydroxy-2-naphthoic acid:tetramethylpyrazine 1:2 cocrystal (1): Typically, 1-hydroxy-2-naphthoic acid (18.8 mg, 0.100 mmol) and tetramethylpyrazine (27.2 mg, 0.200 mmol) were added to a mixture of methanol–distilled-water (5:5 mL) in a 15 mL beaker. The mixture was magnetically stirred continuously for 20 min to form a uniform solution. Then, the above solution was sealed with a sealing film with 15–20 holes and left to stand in air for one hour. Subsequently, the mixture was filtered into another beaker and protected by a membrane with many holes. At room temperature, the mixture was slowly evaporated. In addition, after a few days, single crystals of colorless particles suitable for X-ray diffraction were screened from the mother liquor by a filtration operation. The crystals were dried in a vacuum drying oven. Yield: 77%. Anal. calcd. for $C_{15}H_{14}NO_3$: C, 70.30; H, 5.51; N, 5.47%. Found: C, 73.09; H, 4.80; N, 5.31%. Infrared spectrum (KBr disc, cm^{-1}): 3446 m, 3064 m, 2925 m, 2433 m, 1908 w, 1836 w, 1629 m, 1598 m, 1575 m, 1466 m,1415 m, 1302 m, 1235 s, 1205 m, 1165 s, 1090 m, 909 m, 797 m, 768 m, 754 s, 686 m, 535 m.

1-hydroxy-2-naphthoic acid:1,10-phenanthroline 1:1 cocrystal (2): A methanol solution (5 mL) of 1-hydroxy-2-naphthoic acid (18.8 mg, 0.100 mmol) was added to a stirred distilled-water solution (5 mL) of 1,10-phenanthroline (19.8 mg, 0.100 mmol) in a 15 mL beaker, and the reaction mixture stirred for 20 min to obtain a colorless homogeneous solution. The resulting solution was filtered with qualitative filter paper and covered with a sealing film with 15–20 holes and then held at room temperature in air for a week. Finally, a yellowish flake crystal was formed with a yield of about 85%. Single crystals suitable for X-ray diffraction testing were obtained from the mother liquor by filtration and dried in a vacuum drying oven. Anal. calcd. for $C_{34}H_{24}N_2O_6$: C, 73.37; H, 4.35; N, 5.03%. Found: C, 73.46; H, 4.65; N, 5.12%. Infrared spectrum (KBr disc, cm^{-1}): 3443 m, 3050 m, 1931 w, 1843 w, 1618 m, 1596 m, 1546 m, 1496 m, 1406 m, 1288 m, 1266 w, 1207 w, 1145 m, 1079 m, 1019 m, 965 w, 908 w, 844 m, 801 m, 772 m, 716 m, 463 m.

1-hydroxy-2-naphthoic acid: L2 1:1 cocrystal (3): First, 1-hydroxy-2-naphthoic acid (18.8 mg, 0.100 mmol) was dissolved in methanol (5 mL), to which a distilled-water solution

of L2 (5 mL, 0.200 mmol/mL) was added with stirring for about 15 min in a 15 mL beaker. Second, the mixture solution was percolated into another clean beaker with a sealing film with 15–20 holes and allowed to slowly evaporate at ambient temperature. Ten days later, light yellow, clubbed crystals were prepared. As-prepared single crystals fit for X-ray diffraction were collected from the mother liquor by filtration and dried under vacuum in sequence. Yield: 83%. Anal. calcd. for $C_{18}H_{15}N_2O_3$: C, 70.35; H, 4.92; N, 9.12%. Found: C, 73.51; H, 5.09; N, 8.95%. Infrared spectrum (KBr disc, cm^{-1}): 3440 m, 3137 m, 3041 m, 1919 w, 1631 m, 1583 m, 1507 m, 1496 m, 1411 s, 1363 m, 1306 m, 1276 m, 1215 m, 1154 m, 1083 s, 1026 m, 998 m, 877 m, 830 m, 778 s, 647 s, 579 s, 522 s, 484 s.

2.3. X-ray Crystallography

Cocrystals of 1-hydroxy-2-naphthoic acid were prepared via the corresponding procedure presented above and picked out carefully under a microscope. Then, suitable single crystals were individually well-fixed on a glass pip for single-crystal X-ray diffraction analysis. Intensity data were collected using a Siemens Smart CCD diffractometer equipped with a normal-focus, 2.4 kW sealed-tube X-ray source (graphite-monochromatic MoKa radiation (l = 0.71073 Å)) operating at 50 kV and 40 mA. The crystal structures were solved by direct methods using SHELXS-97 and refined using full-matrix least-squares techniques based on F^2 with the SHELXL-97 crystallographic software package [46]. The hydrogen atoms were placed at calculated positions and refined as riding atoms with isotropic displacement parameters. The crystallographic parameters of all the complexes are summarized in Table 1. CCDC reference numbers 1497090–1497092 contain the supplementary crystallographic data.

Table 1. Crystallographic parameters of structures 1–3.

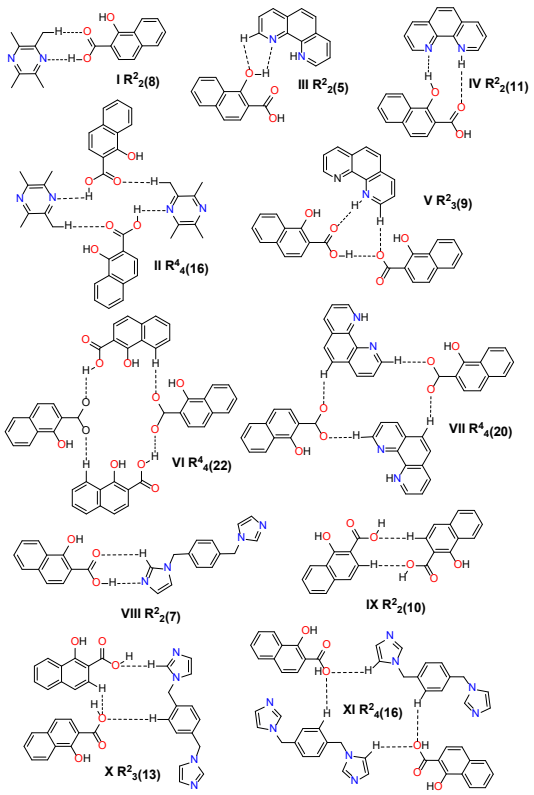
	1	**2**	**3**
Empirical formula	C15H14NO3	C34H24N2O6	C18H15N2O3
M	256.27	556.55	307.32
Crystal system	Monoclinic	Monoclinic	Monoclinic
Space group	P21/c	P21/c	P21/c
a/Å	7.5979(3)	7.5531(3)	8.6933(3)
b/Å	20.1355(9)	32.7203(13)	9.2525(3)
c/Å	8.7223(5)	11.3535(5)	18.8769(5)
α/deg	90	90	90
β/deg	106.485(5)	104.298(5)	97.675(3)
γ/deg	90	90	90
V/Å3	1279.55(11)	2719.0(2)	1504.76(8)
Z	4	4	4
ρcalcd. (g/cm^3)	1.330	1.360	1.357
μ (mm^{-1})	0.093	0.094	0.094
F(000)	540.0	1160.0	644.0
Total/independent reflections	5423/2248	11,914/4770	8030/3556
Data/restraints/parameters	2248/0/176	4770/1/385	3556/1/213
Rint	0.0251	0.0296	0.0222
R,a Rwb	0.0526, 0.1577	0.0449, 0.1124	0.0502, 0.1339
GOF	1.053	1.011	0.875

3. Results and Discussion

3.1. Molecular and Supramolecular Structural Descriptions of Compounds **1**–**3**

To guide the selection process of the suitable co-formers, we altered the molar ratio of 1-hydroxy-2-naphthoic acid to each N-containing heterocycle (1:2, 1:1, and 2:1) in our initial parallel experiments. Two solvents of methanol and water with different polarities were chosen. Finally, we successfully prepared three new cocrystals of 1-hydroxy-2-naphthoic acid with tetramethylpyrazine **1**, 1,10-phenanthroline **2**, and L2 [1,4-bis(imidazol) dimethylbenzene] **3.** These solid phases involving 1-hydroxy-2-naphthoic acid and N-heterocycles

were identified by single-crystal X-ray diffraction, FT–IR spectroscopy, and thermogravimetric analysis (TGA). The crystal structures of cocrystals **1–3** involved wide hydrogen bond networks, in which the 1-hydroxy-2-naphthoic acid and base components generated a series of possible synthons, which are exhibited in Scheme 2. The distances and angles of the primary hydrogen bonds of cocrystals **1–3** are listed in Table 2. The variations in the hydrogen bonding interactions of the three structures will be discussed separately in the following sections.



Scheme 2. Various hydrogen bonding synthons observed in the crystal structures of 1-hydroxy-2-naphthoic acid cocrystals.

Table 2. Hydrogen bond metrics for complexes **1–3**.

Compounds	D-H···A (Å)	D-H(Å)	H···A(Å)	D···A(Å)	D-H···A (Deg)
1	O3–H3···N1 [a]	0.82	1.93	2.701	156
	C19–H19B···O2 [a]	0.96	2.71	3.505	141
	N1–H1···O4 [b]	0.86	1.97	2.780	157
2	O6–H6···N2 [c]	0.82	2.55	3.053	121
	C27–H27···O6 [b]	0.93	2.49	3.091	123
	C28–H28···O5 [b]	0.93	2.63	3.457	149
	O5–H5···O1 [c]	1.13	1.34	2.464	172
	C35–H35···O3 [d]	0.93	2.51	3.436	177
	C22–H22···O1 [e]	0.93	2.77	3.669	163
3	O1–H1···N2 [c]	0.88	1.67	2.548	176
	C20–H20···O1 [e]	0.93	2.64	3.495	153
	C17–H17A···O3 [e]	0.97	2.49	3.157	126

[a] x, 0.5−y, −0.5 + z; [b] x, y, z; [c] −x, −y, −z; [d] x, −1 + y, z; [e] x, y, −1 + z.

1-hydroxy-2-naphthoic acid-tetramethylpyrazine cocrystal 1. Complex **1** crystallized as colorless, granular crystals in a 1:2 molar ratio of 1-hydroxy-2-naphthoic acid and tetramethylpyrazine. The structural determination showed that compound **1** formed a cocrystal in the monoclinic $P2_1/c$ space group with Z = 4. As described in Figure 1a, the

asymmetric unit consisted of a neutral 1-hydroxy-2-naphthoic acid molecule and half a neutral tetramethylpyrazine molecule. Within each 1-hydroxy-2-naphthoic acid molecule, the angle between the carboxyl group plane and the naphthalene ring plane was 8.875(139)°. The dihedral angle between the naphthalene ring of the acid molecule and the pyrazine ring of the base molecule was 4.944(48)°.

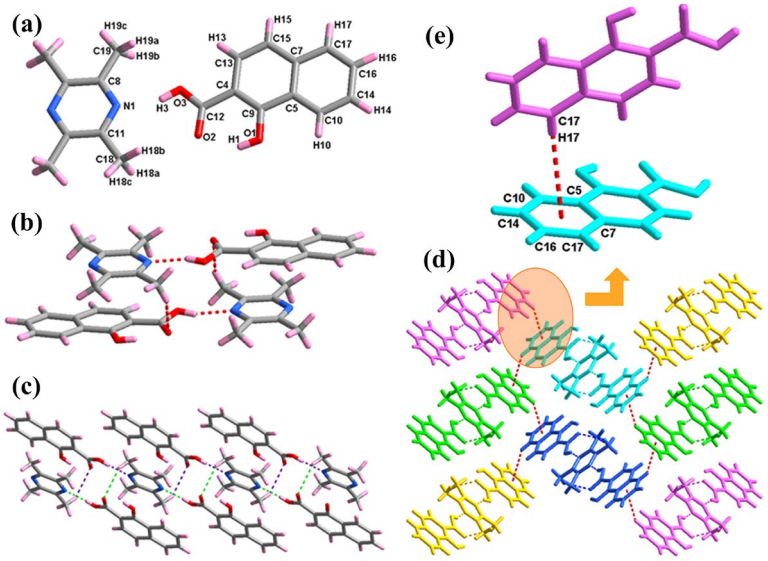


Figure 1. (**a**) Molecular structure of complex 1 with atom labeling of the asymmetric units; (**b**) synthon II $R_4^4(16)$ between 1-hydroxy-2-naphthoic acid and tetramethylpyrazine; (**c**) one-dimensional chain via synthon $R_4^4(16)$; (**d**) three-dimensional network via weak C–H···π interactions (adjacent chains are expressed as different colors); (**e**) the C–H···π interactions. (O, red; N, light blue; C, gray; H, rose, in this and subsequent figures).

At first, two molecules of tetramethylpyrazine and two molecules of 1-hydroxy-2-naphthoic acid were self-assembled to form a stable tetramer through a pair of strong hydrogen bonds $_{O3}$–H_3···N_1 (2.70 Å) and a pair of weak hydrogen bonds C_{19}–H_{19}B···O_2 (3.51 Å) with an $R_4^4(16)$ motif (synthon II) (shown in Figure 1b). Then, adjacent $R_4^4(16)$ synthons combined to form a one-dimensional chain by sharing their tetramethylpyrazine molecules (shown in Figure 1c). Further analysis of the crystal packing of **1** showed that the neighboring 1D chains were connected each other in a 3D supramolecular network via weak C–H···π interactions between the naphthalene rings of the acid molecules along the crystallographic axis (see Figure 1d). The distance of the C17–H17···π stacking between the C_{17} and the centroid Cg of the aromatic group C10, C5, C7, C17, C16, and C14 was 3.81 Å, as shown in Figure 1e. The angle of C17–H17···Cg was approximately 142°. Meanwhile, another small ring motif, I $R_2^2(8)$, was observed in this structure.

1-hydroxy-2-naphthoic acid–1,10-phenanthroline cocrystal 2. The structural determination of compound **2** indicated that cocrystal **2** crystallized in space group $P2_1/c$ with Z = 4 and possessed a crystallographically independent 1,10-phenanthroline monocation, one 1-hydroxy-2-naphthoic acid monoanion, and a 1-hydroxy-2-naphthoic acid neutral molecule (Figure 2a). In the above structure, the dihedral angles between the aryl ring plane of the 1-hydroxy-2-naphthoic acids and the 1,10-phenanthroline ring were 8.459(99)° and 63.664(54)°, respectively. Furthermore, the dihedral angle between the two naphthalene rings was 62.804(59)°. Within each neutral acid molecule, the carboxyl plane formed a dihedral angle of 4.351(79)° with the naphthalene ring plane. The carboxyl plane formed a dihedral angle of 9.241(186)° with the naphthalene ring in each 1-hydroxy-2-naphthoic acid anion.

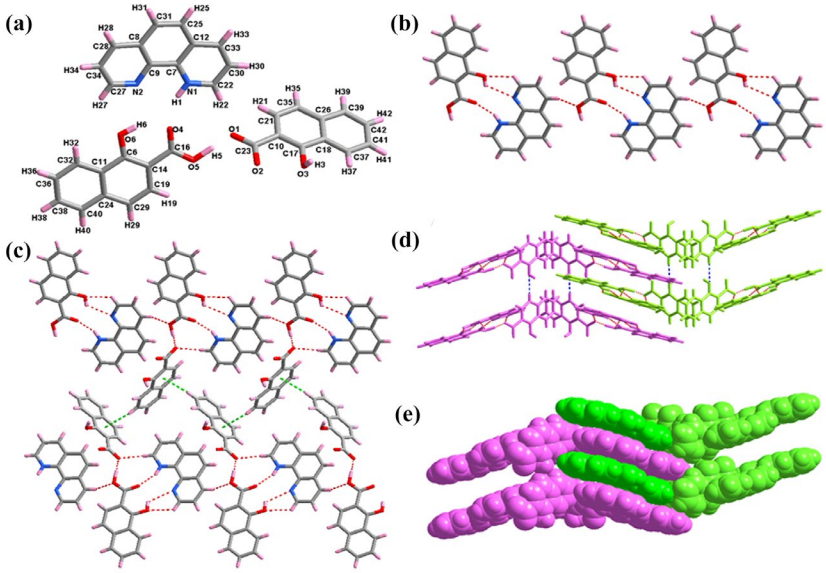


Figure 2. (**a**) Molecular structure of complex 2 with atom labeling of the asymmetric units; (**b**) 1D banded structure including acid and base subunits; (**c**) 2D layer structure linked by hydrogen bonds and C–H···π interactions; (**d**) 3D multilayer structure connected via C–H···O hydrogen bonds and stabilized by π···π stacking; (**e**) space-filling model of the 3D network.

As shown in Figure 2b, the acid molecules and base molecules were held together through three hydrogen bonds, namely N1–H1···O4, O6–H6···N2, and C27–H27···O6, together creating synthons III $R^2_2(5)$ and IV $R^2_2(11)$, resulting in a dimer motif. These dimer motifs were linked through weak hydrogen bonds at C28–H28···O5 (3.46 Å) to form a one-dimensional banded chain along the *a* axis. The acid anions and 1D chains were linked together through hydrogen bonds at O5–H5···O1 (2.46 Å) and C22–H22···O1 (3.16 Å), and, meanwhile, the acid anions interacted with each other through C–H···π interactions, which gave rise to a 2D layer (see Figure 2c). The distance of the C14-H14···π interaction between the C14 and the centroid Cg of the aromatic group C10, C17, C18, C26, C35, and C21 was 3.73 Å. The angle of C14-H14···Cg was about 151°. As illustrated in Figure 2d,e, the 2D layers were connected via C35–H35···O3 hydrogen bonds to generate a 3D multilayer structure, which was further fixed by the face-to-face π···π stacking interactions between the 1-hydroxy-2-naphthoic acid and 1,10-phenanthroline. In the 3D array, three kinds of synthons, namely V $R_2{}^3(9)$, VI $R_4{}^4(22)$, and VII $R_4{}^4(20)$, were observed.

1-hydroxy-2-naphthoic acid–L2 cocrystal 3. Regarding complex **3**, the structural determination proved that it was an acentric two-component molecular crystal (space group $P2_1/c$, Z = 4), in which each 1-hydroxy-2-naphthoic acid molecule crystallized with half an L2 molecule (Figure 3a). In each L2 molecule, the dihedral angles between the two terminal imidazole rings and the central benzene ring were all 81.588°. The plane of the carboxyl group formed a dihedral angle of 2.048° with the plane of the naphthalene ring in each 1-hydroxy-2-naphthoic acid subunit, and the dihedral angle between the naphthalene ring and the aromatic ring of L2 was 45.482°.

The analysis of the crystal packing for cocrystal **3** reflected that the co-formers were connected in a 1D linear chain through two types of hydrogen bonds: O1–H1···N2 (2.55 Å, 176°) and C22–H22···O1 (3.67 Å, 163°) (as shown in Figure 3b; for the sake of clarity, partial C–H H atoms are omitted in Figure 3b). The above-involved one-dimensional chains were further connected by C20–H20···O1 (3.50 Å, 153°) and C17–H17A···O3 (3.16 Å, 126°) hydrogen bonds to form a 3D tessellate-type supramolecular architecture (see Figure 3c). Consequently, hydrogen-bonded patterns marked as synthons VIII $R_2{}^2(7)$, IX $R_2{}^2(10)$, X $R_2{}^3(13)$, and XI $R_2{}^4(16)$ were formed. Impressively, the pyridine–carboxylic acid synthon VIII $R_2{}^2(7)$ is considered to be the best combination between a hydrogen-bonding donor and acceptor due to its stability and reliability, which has been certified to be an efficient

tool in the formation of predictable hydrogen-bonding networks. Recent reports have shown that this synthon is easily formed between carboxylic acid and pyridine groups due to its relatively low energy. When neither of the two competing functional groups is present, the probability of this synthon formating is about 90% [38].

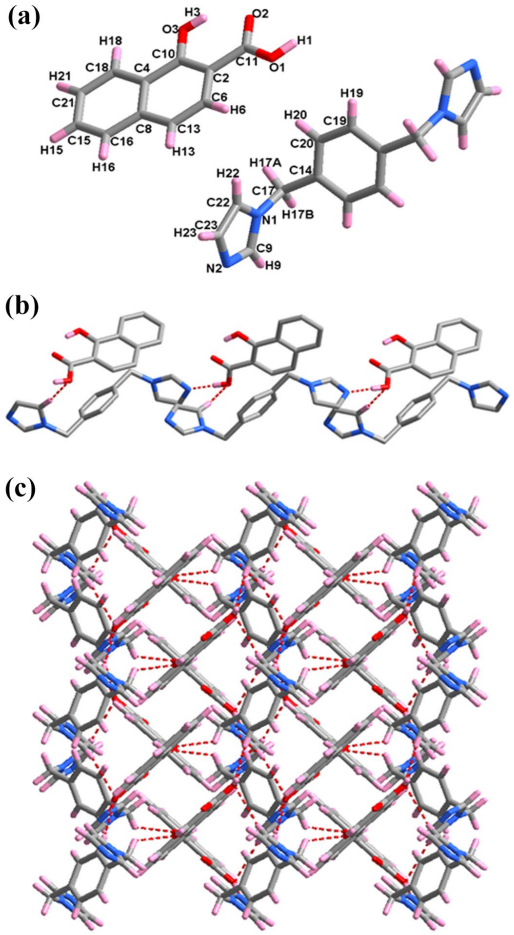


Figure 3. (**a**) Molecular structure of complex 3 with atom labeling of the asymmetric units; (**b**) 1D chain via O–H···N and C–H···O hydrogen bonds; (**c**) 3D tessellate-type supramolecular network via two types of C–H···O hydrogen bonds. For the sake of clarity, partial C–H H atoms are omitted in (**b**).

3.2. Thermal Stability

Compounds **1–3** were stable in air and could maintain their structural integrity for long periods of time under environmental conditions. Thermogravimetric analysis (TGA) was performed to study the thermal stability of the single components, the mechanically ground mixtures, and these crystalline materials between 50 and 500 °C under a noble gas (N_2 atmosphere). As shown in Figure 4, the TGA curves of complexes **1** and **2** showed single weight losses. Complex **1** decomposed from 133 °C to 225 °C (peaking at 198 °C), while complex **2** was more stable than complex **1,** and the decomposition of its framework began at 146 °C (peaking at 213 °C). The TGA curve of complex **3** showed two consecutive weight losses from 112 °C to 348 °C (peaking at 132 °C and 230 °C, respectively). As for complex **3**, the first weight loss of 37% from 112 °C to 145 °C corresponded to the decomposition of L2 molecules (calculated: 42%). The second weight loss of 63% (calculated: 58%) was due to the decomposition of the 1-hydroxy-2-naphthoic acid molecules.

The thermal stability of the pure components and the mechanical mixtures were investigated by thermogravimetric analysis (TGA) experiments. The TGA curves of the pure components are given in Figure 5a. During the heating process, tetramethylpyrazine, 1,10-phenanthroline, 1,4-bis(imidazol) dimethylben-zene, and 1-hydroxy-2-naphthoic acid were

stable up to 213.4, 271.6, 63.9, and 183.9 °C, respectively, which was due to the decomposition of the tetramethylpyrazine, 1,10-phenanthroline, 1,4-bis(imidazol) dimethylben-zene, and 1-hydroxy-2-naphthoic acid. For 1,10-phenanthroline, the TGA curve showed a first weight loss of 8.14% from 34.7 °C to 64.3 °C, corresponding to the loss of the guest water molecules caused by the sample's moisture absorption. The second weight loss occurred in the range of 271.6–390.0 °C, which was due to the decomposition of the 1,10-phenanthroline molecules. The analyses of the mechanical mixtures are shown in Figure 5b. After mechanical grinding, the general trend of their thermogravimetry was consistent with that shown in Figure 4, and the slight difference may be due to solid-phase reactions caused by grinding.

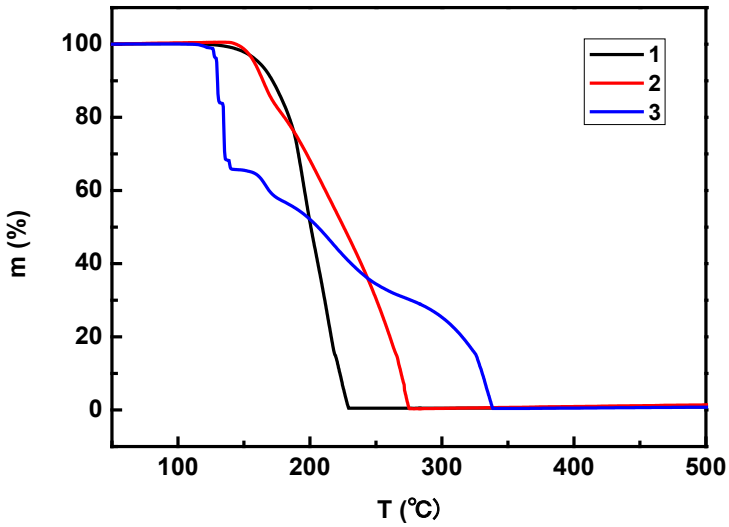


Figure 4. The thermogravimetric analysis for compounds **1**–**3**.

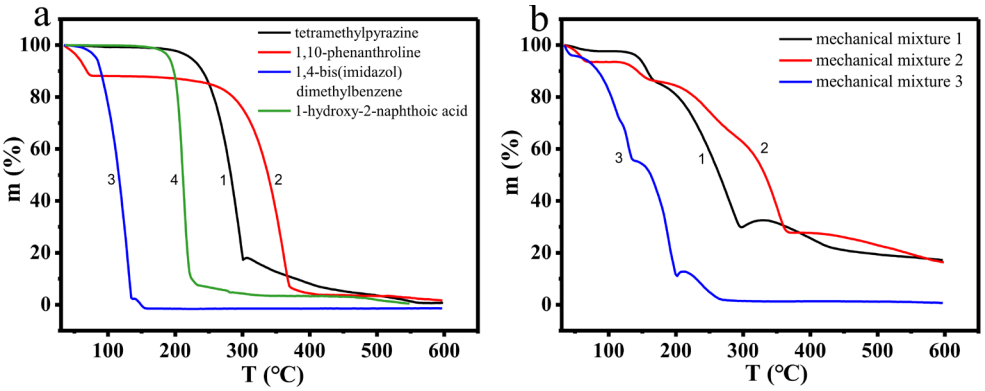


Figure 5. The thermogravimetric analysis for pure components and mechanical mixtures.

3.3. FT–IR

The IR spectroscopy of compound **1** is shown in Figure S1. The wide and strong absorption peak at 3446 cm^{-1} was attributed to the stretching vibrations of O–H. The absorption peaks at 3064 cm^{-1} and 3012 cm^{-1} were caused by the stretching vibrations of the C–H bonds on the aromatic ring. Symmetric contraction vibrations and antisymmetric contraction vibrations, which were classified as methyl (–CH_3), were absorbed at 2853 cm^{-1} and 2925 cm^{-1}. The stretching vibrations of the C=O bond in the carboxyl group appeared at 1694 cm^{-1}. The four sharp and strong absorption peaks between 1629 cm^{-1} and 1466 cm^{-1} were attributed to the deformation and vibrations of the skeleton of the aromatic ring. The strong absorption peak between 1235 cm^{-1} and 1165 cm^{-1} may have been due to C–N or C=N stretching vibrations. The presence of weak and broad bands

in the 2500–2600 cm^{-1} and 1800–1900 cm^{-1} spectral range was observed, which were assigned to O–H···N hydrogen bonds [47,48].

The IR spectroscopy of compound **2** (Figure S2) showed an absorption peak at 3443 cm^{-1}, which may have been due to the stretching vibrations of the hydroxyl group (O–H) in the compound or the N–H stretching vibrations of the organic amine. The contraction vibrations of the C–H bonds in the aromatic ring appeared near 3050 cm^{-1}. The five medium and strong absorption peaks at 1618, 1596, 1546, 1469, and 1453 cm^{-1} were due to the skeleton deformation vibrations of aromatic ring. The absorption peak between 908 cm^{-1} and 659 cm^{-1} was attributed to the bending vibrations of the C–H bonds on the aromatic ring.

The IR spectroscopy of compound **3** (Figure S3) showed that the wide and strong absorption peak at 3440 cm^{-1} was caused by the stretching vibrations of the O–H bonds in the aromatic ring of the compound. The absorption peaks at 3137 cm^{-1} and 3041 cm^{-1} belonged to the stretching vibrations of the C–H bonds on the aromatic ring. The weaker absorption peaks at 2954 cm^{-1} and 2928 cm^{-1} were classified as the symmetric and antisymmetric stretching vibrations of methylene (–CH_2–). Several sharp and strong absorption peaks between 1631 cm^{-1} and 1411 cm^{-1} were attributed to the deformation and vibrations of the skeleton of the aromatic ring. The absorption peak between 1306 cm^{-1} and 1083 cm^{-1} may have been due to C-N or C=N stretching vibrations.

4. Conclusions

In summary, we successfully synthesized three novel molecular cocrystals by a solvent evaporation technique. They all belonged to a group of 1-hydroxy-2-naphthoic acid molecule cocrystals containing N-heteroaromatic compounds and were further analyzed by single-crystal X-ray diffraction testing. It was distinctly observed in all the three structures that weak forces (C–H···O, C–H···π interactions) also played a major role in the process of their self-assembly, as well as strong and conventional hydrogen bonds (N–H···O/O–H···N/O–H···O), once the stronger hydrogen bonds were all well utilized and consumed. The analysis of the supramolecular synthons in the existing structures demonstrated that the occurrence of the robust and common synthon $R_2^2(7)$ was again observed in cocrystal **3**. In addition, other several small- and large-sized ring motifs were also observed in the present structures studied in this manuscript, such as $R_2^2(5)$, $R_2^2(7)$, $R_2^2(8)$, $R_2^3(13)$, $R_2^4(16)$, $R_4^4(16)$, $R_4^4(22)$, and so on. Our systematic studies here also demonstrated that hydroxynaphthalic acids are an excellent candidate for constructing supramolecular structures with organic amines.

Supplementary Materials: The following supporting information can be downloaded at: https://www.mdpi.com/article/10.3390/cryst13030402/s1, Figure S1: The IR curve of 1; Figure S2: The IR curve of 2; Figure S3: The IR curve of 3; Figure S4: DSC curve of (a−c) compounds **1**−**3** and (d−f) mechanical mixtures.

Author Contributions: Conceptualization, H.Q. and K.L.; methodology, Y.M.; software, N.L.; validation, Y.M.; formal analysis, M.Z.; data curation, K.L.; writing—original draft preparation, H.Q.; writing—review and editing, R.C.; visualization, Y.Y.; supervision, Z.L.; funding acquisition, K.L. All authors have read and agreed to the published version of the manuscript.

Funding: This research was funded by the Natural Science Foundation of Shandong Province, China (No. ZR2022MB022) and the National Natural Science Foundation of China (52072197 and 52272222).

Data Availability Statement: The data that support the findings of this study are available from the corresponding author, (K.L.), upon reasonable request.

Conflicts of Interest: The authors declare no conflict of interest.

References

1. Desiraju, G.R. Crystal engineering: From molecule to crystal. *J. Am. Chem. Soc.* **2013**, *135*, 9952–9967. [CrossRef] [PubMed]
2. Boese, R.; Bläser, D.; Jansen, G. Synthesis and theoretical characterization of an acetylene-ammonia cocrystal. *J. Am. Chem. Soc.* **2009**, *131*, 2104–2106. [CrossRef] [PubMed]
3. Cinčić, D.; Friščić, T.; Jones, W. A stepwise mechanism for the mechanochemical synthesis of halogen-bonded cocrystal architectures. *J. Am. Chem. Soc.* **2008**, *130*, 7524–7525. [CrossRef] [PubMed]
4. Mandala, V.S.; Loewus, S.J.; Mehta, M.A. Monitoring cocrystal formation via in situ solid-state NMR. *J. Phys. Chem. Lett.* **2014**, *5*, 3340–3344. [CrossRef]
5. Zhang, T.; Yang, Y.; Zhao, X.; Jia, J.; Su, H.; He, H.; Gu, J.; Zhu, G. Dissolution and pharmacokinetic properties of two paliperidone cocrystals with 4-hydroxybenzoic and 4-aminobenzoic acid. *CrystEngComm* **2014**, *16*, 7667–7672. [CrossRef]
6. Sugandha, K.; Kaity, S.; Mukherjee, S.; Isaac, J.; Ghosh, A. Solubility enhancement of ezetimibe by a cocrystal engineering technique. *Cryst. Growth Des.* **2014**, *14*, 4475–4486. [CrossRef]
7. Aitipamula, S.; Banerjee, R.; Bansal, A.K.; Biradha, K.; Cheney, M.L.; Choudhury, A.R.; Desiraju, G.R.; Dikundwar, A.G.; Dubey, R.; Duggirala, N.; et al. Polymorphs, salts, and cocrystals: What's in a name. *Cryst. Growth Des.* **2012**, *12*, 2147–2152. [CrossRef]
8. Wheeler, S.E.; Seguin, T.J.; Guan, Y.F.; Doney, A.C. Noncovalent interactions in organocatalysis and the prospect of computational catalyst design. *Acc. Chem. Res.* **2016**, *49*, 1061–1069. [CrossRef]
9. Riffet, V.; García, J.C.; Carrasco, J.; Calatayud, M. Alkali ion incorporation into V_2O_5: A noncovalent interactions analysis. *J. Phys. Chem. C* **2016**, *120*, 4259–4265. [CrossRef]
10. Dethlefs, K.M.; Hobza, P. Noncovalent interactions: A challenge for experiment and theory. *Chem. Rev.* **2000**, *100*, 143–167. [CrossRef]
11. Johnson, E.R.; Keinan, S.; Sánchez, P.M.; García, J.C.; Cohen, A.J.; Yang, W.T. Revealing noncovalent interactions. *J. Am. Chem. Soc.* **2010**, *132*, 6498–6506. [CrossRef]
12. Sharma, C.V.K.; Clearfield, A. Three-dimensional hexagonal structures from a novel self-complementary molecular building block. *J. Am. Chem. Soc.* **2000**, *122*, 4394–4402. [CrossRef]
13. Aakeröy, C.B.; Chopade, P.D.; Ganser, C.; Desper, J. Facile synthesis and supramolecular chemistry of hydrogen bond/halogen bond-driven multi-tasking tectons. *Chem. Commun.* **2011**, *47*, 4688–4690. [CrossRef]
14. Wang, L.; Xue, R.; Xu, L.; Lu, X.; Chen, R.; Tao, X. Hydrogen-bonding directed cocrystallization of flexible piperazine with hydroxybenzoic acid derivatives: Structural diversity and synthon prediction. *Sci. China. Chem.* **2012**, *55*, 1228–1235. [CrossRef]
15. Desiraju, G.R. Reflections on the hydrogen bond in crystal engineering. *Cryst. Growth Des.* **2011**, *11*, 896–898. [CrossRef]
16. Wagner, B.D. Hydrogen bonding of excited states in supramolecular host–guest inclusion complexes. *Phys. Chem. Chem. Phys.* **2012**, *14*, 8825–8835. [CrossRef] [PubMed]
17. Wang, L.; Hu, Y.; Wang, W.; Liu, F.; Huang, K. Energetic multi-component molecular solids of tetrafluoroterephthalic acid with some aza compounds by strong hydrogen bonds and weak intermolecular interactions of C-H/F and C-H/O. *CrystEngComm* **2014**, *16*, 4142–4161. [CrossRef]
18. Schultheiss, N.; Lorimer, K.; Wolfe, S.; Desper, J. Molecular networks created by charge-assisted hydrogen bonding in phosphonate; phosphate; and sulfonate salts of bis(amidines). *CrystEngComm* **2010**, *12*, 742–749. [CrossRef]
19. Tsai, S.C.; Lin, Y.C.; Lin, E.L.; Chiang, Y.W.; Kuo, S.W. Hydrogen bonding strength effect on self-assembly supramolecular structures of diblock copolymer/homopolymer blends. *Polym. Chem.* **2016**, *7*, 2395–2409. [CrossRef]
20. Jones, A.O.F.; Leech, C.K.; McIntyre, G.J.; Wilson, C.C.; Thomas, L.H. Engineering short; strong hydrogen bonds in urea di-carboxylic acid complexes. *CrystEngComm* **2014**, *16*, 8177–8184. [CrossRef]
21. Dai, Z.H.; Qiang, L.; Tang, L.M.; Guo, B.H. A novel supramolecular polymer fabricated via stronger hydrogen-bonding interactions between substituted amide groups: Design; synthesis; properties and mechanism. *RSC Adv.* **2015**, *5*, 84104–84112. [CrossRef]
22. Nishio, M.; Umezawa, Y.; Fantini, J.; Weiss, M.S.; Chakrabarti, P. CH-p hydrogen bonds in biological macromolecules. *Phys. Chem. Chem. Phys.* **2014**, *16*, 12648–12683. [CrossRef] [PubMed]
23. Helttunen, K.; Lehtovaara, L.; Häkkinen, H.; Nissinen, M. Crystal structures and density functional theory calculations of o- and p-Nitroaniline derivatives: Combined effect of hydrogen bonding and aromatic interactions on dimerization energy. *Cryst. Growth Des.* **2013**, *13*, 3603–3612. [CrossRef]
24. Tiefenbacher, K.; Rebek, J. Selective stabilization of self-assembled hydrogen-bonded molecular capsules through $\pi-\pi$ interactions. *J. Am. Chem. Soc.* **2012**, *134*, 2914–2917. [CrossRef] [PubMed]
25. Altheimer, B.D.; Pagola, S.; Zeller, M.; Mehta, M.A. Mechanochemical conversions between crystalline polymorphs of a complex organic solid. *Cryst. Growth Des.* **2013**, *13*, 3447–3453. [CrossRef]
26. Loots, L.; Wahl, H.; Westhuizen, L.; Haynes, D.A.; Roex, T. Interconversion between different stoichiometric forms of a three-component crystal via liquid-assisted grinding. *Chem. Commun.* **2012**, *48*, 11507–11509. [CrossRef]
27. Tothadi, S.; Joseph, S.; Desiraju, G.R. Synthon modularity in cocrystals of 4-bromobenzamide with n-alkanedicarboxylic acids: Type I and type II halogen···halogen interactions. *Cryst. Growth Des.* **2013**, *13*, 3242–3254. [CrossRef]
28. Prohens, R.; Portell, A.; Font-Bardia, M.; Bauzá, A.; Frontera, A. Experimental and theoretical study of aromaticity effects in the solid state architecture on squaric acid derivatives. *Cryst. Growth Des.* **2014**, *14*, 2578–2587. [CrossRef]

29. Kim, K.S.; Karthikeyan, S.; Singh, N.J. How different are aromatic π interactions from aliphatic π interactions and non-π stacking interactions? *J. Chem. Theory Comput.* **2011**, *7*, 3471–3477. [CrossRef]
30. Putta, A.; Mottishaw, J.D.; Wang, Z.H.; Sun, H. Rational design of lamellar π-π stacked organic crystalline materials with short interplanar distance. *Cryst. Growth Des.* **2014**, *14*, 350–356. [CrossRef]
31. Smith, M.G.; Lemmerer, A. The photodimerization of Schiff bases: Synthesis and crystal structures of benzophenone azines and their weak CH···π interactions. *J. Mol. Struct.* **2019**, *1179*, 132–144. [CrossRef]
32. Krishna, G.R.; Devarapalli, R.; Lal, G.; Redd, C.M. Mechanically flexible organic crystals achieved by introducing weak interactions in structure: Supramolecular shape synthons. *J. Am. Chem. Soc.* **2016**, *138*, 13561–13567. [CrossRef]
33. Ebenezer, S.; Muthiah, P.T. Design of co-crystals/salts of aminopyrimidines and carboxylic acids through recurrently occurring synthons. *Cryst. Growth Des.* **2012**, *12*, 3766–3785. [CrossRef]
34. Hathwar, V.R.; Thakur, T.S.; Dubey, R.; Pavan, M.S.; Guru, R.T.N.; Desiraju, G.R. Extending the supramolecular synthon based fragment approach (SBFA) for transferability of multipole charge density parameters to monofluorobenzoic acids and their cocrystals with isonicotinamide: Importance of C-H···O.; C-H···F; and F···F intermolecular regions. *J. Phys. Chem. A* **2011**, *115*, 12852–12863. [PubMed]
35. Khan, M.; Enkelmann, V.; Brunklaus, G. Heterosynthon mediated tailored synthesis of pharmaceutical complexes: A solid-state NMR approach. *CrystEngComm* **2011**, *13*, 3213–3223. [CrossRef]
36. Sanphui, P.; Babu, N.J.; Nangia, A. Temozolomide cocrystals with carboxamide coformers. *Cryst. Growth Des.* **2013**, *13*, 2208–2219. [CrossRef]
37. Ivasenko, O.; Perepichka, D.F. Mastering fundamentals of supramolecular design with carboxylic acids. Common lessons from X-ray crystallography and scanning tunneling microscopy. *Chem. Soc. Rev.* **2011**, *40*, 191–206. [CrossRef] [PubMed]
38. Wang, L.; Xu, L.; Xue, L.; Lu, X.; Chen, R.; Tao, X. Cocrystallization of N-donor type compounds with 5-sulfosalicylic acid: The effect of hydrogen-bonding supramolecular architectures. *Sci. China Chem.* **2012**, *55*, 138–144. [CrossRef]
39. Duggirala, N.K.; Wood, G.P.; Fischer, A.; Wojtas, Ł.; Perry, M.L.; Zaworotko, M.J. Hydrogen bond hierarchy: Persistent phenol···chloride hydrogen bonds in the presence of carboxylic acid moieties. *Cryst. Growth Des.* **2015**, *15*, 4341–4354. [CrossRef]
40. Xing, P.; Li, Q.; Li, Y.; Wang, K.; Zhang, Q.; Wang, L. Organic salts formed by 2,4,6-triaminopyrimidine and selected carboxylic acids via a variety of hydrogen bonds: Synthons cooperation; and crystal structures. *J. Mol. Struct.* **2017**, *1136*, 59–68. [CrossRef]
41. Mukherjee, A.; Desiraju, G.R. Combinatorial exploration of the structural landscape of acide-pyridine cocrystals. *Cryst. Growth Des.* **2014**, *14*, 1375–1385. [CrossRef]
42. Ejarque, D.; Calvet, T.; Font-Bardia, M.; Pons, J. Cocrystals Based on 4,4′-bipyridine: Influence of Crystal Packing on Melting Point. *Crystals* **2021**, *11*, 191. [CrossRef]
43. Cruz-Cabeza, A.J. Acid–base crystalline complexes and the p K a rule. *CrystEngComm* **2012**, *14*, 6362–6365. [CrossRef]
44. Braga, D.; Grepioni, F. Reactions Between or Within Molecular Crystals. *Angew. Chem. Int. Ed.* **2004**, *43*, 4002–4011. [CrossRef] [PubMed]
45. Hoskins, B.F.; Robson, R.; Slizys, D.A. An infinite 2D polyrotaxane network in $Ag_2(bix)_3(NO_3)_2$ (bix = 1;4-Bis(imidazol-1-ylmethyl)benzene). *J. Am. Chem. Soc.* **1997**, *119*, 2952–2953. [CrossRef]
46. Sheldrick, G.M. *SHELXS-97. Program for the Solution of Crystal Structures*; University of Göttingen: Göttingen, Germany, 1997.
47. Zaltariov, M.F.; Cazacu, M.; Shova, S.; Vlad, A.; Stoica, L.; Hamciuc, E. Hydrogen-bonded supramolecular polymers containing dimethylsilane groups: Synthesis, crystal structure, and characterization. *J. Polym. Sci. Pol. Chem.* **2012**, *50*, 3775–3787. [CrossRef]
48. Zaltariov, M.F.; Filip, D.; Varganici, C.D.; Macocinschi, D. ATR-FTIR and thermal behavior studies of new hydrogel formulations based on hydroxypropyl methylcellulose/poly (acrilic acid) polymeric blends. *Cell. Chem. Technol.* **2018**, *52*, 619–631.

Disclaimer/Publisher's Note: The statements, opinions and data contained in all publications are solely those of the individual author(s) and contributor(s) and not of MDPI and/or the editor(s). MDPI and/or the editor(s) disclaim responsibility for any injury to people or property resulting from any ideas, methods, instructions or products referred to in the content.